Optica Applicata, Vol. LIV, No. 3, 2024
DOI: 10.37190/oa240305

Exploring a novel turbulence model: The Chi-square/inverse Gamma approach for enhanced free space optics (FSO) communication

NENAD STANOJEVIĆ[1,*], ĐOKO BANĐUR[1], LAZAR MOSUROVIĆ[2], PETAR SPALEVIĆ[1], STEFAN PANIĆ[3,*]

[1]Faculty of Technical Sciences, University of Priština – Kosovska Mitrovica, Knjaza Miloša 7, 38220 Kosovska Mitrovica, Serbia

[2]Faculty of Economics and Engineering, University of Business Academy – Novi Sad, Cvećarska 2, 21107 Novi Sad, Serbia

[3]Faculty of Sciences, University of Priština – Kosovska Mitrovica, Lole Ribara 29, 38220 Kosovska Mitrovica, Serbia

Corresponding authors: Nenad Stanojević – nenads25@gmail.com , Stefan Panić - stefan.panic@pr.ac.rs

The manuscript introduces a novel turbulence model for free space optics (FSO) communication, constructed through the amalgamation of two distinct statistical models, rooted in the scintillation theory. A closed-form expression for the probability density function (PDF) and cumulative distribution function (CDF) of the turbulence channel, specifically the Chi-square/inverse Gamma distribution, was deduced. Further the influence of zero boresight pointing errors on the performances of FSO transmission over the obtained atmospheric turbulence channel has been considered. To delve into the intricacies of the channel, an examination of the average bit error rate (ABER) was undertaken as an evaluative metric for the transmitted signal's quality. The ABER analysis was specifically conducted within the framework of IM/DD (intensity modulation and direct detection) and OOK (on-off keying), considering diverse sets of system parameters and across various turbulence scenarios. In the same manner, ABER analysis has been carried out for the subcarrier intensity modulation (SIM) with differential phase-shift keying (DPSK).

Keywords: turbulence modelling, free space optics (FSO), Chi-square/inverse Gamma distribution, scintillation theory, average bit error rate (ABER).

1. Introduction

Transmitting high-resolution data through FSO systems offers notable advantages, including high transmission speeds (up to 30 Gbps), directional beam characteristics, im-

munity to electromagnetic radiation, use of unlicensed frequency spectrum, flexibility, low implementation costs, and enhanced security. However, drawbacks exist, such as potential interference. The directed optical beam's propagation may result in signal attenuation due to atmospheric turbulence and transmitter/receiver pointing errors. Transmission delays induced by these factors can lead to information transmission errors, affecting the accuracy of transmitted bits (bit error rate – BER). In addition to atmospheric turbulence, pointing errors represent another factor contributing to signal degradation in FSO systems. These errors result from misalignment between the transmitted signal and the receiving detector [1]. The zero boresight transmission model delineates misalignment error, incorporating factors such as the radius of the optical beam at a specific distance from the transmitter, the diameter of the circular detector's aperture, and variations in surface tilt.

Mathematical models play a crucial role in delineating the statistical characteristics of FSO signal intensity, essentially capturing the signal's behaviour. The most commonly used mathematical models for fluctuations of optical signals in a turbulent channel are: log-normal [2,3], Gamma-Gamma [4-6], model with a negative exponent [7,8], Nakagami [5,9], Rician model [10,11]. Under conditions of mild turbulence in clear skies, the log-normal distribution emerges as the most appropriate choice [12,13]. The Gamma-Gamma distribution is widely adopted in the literature due to its consistent alignment with theoretical and experimental results, proving effective across a diverse array of atmospheric turbulence scenarios [4,14]. These models collectively account for the simultaneous influence of eddy fluctuations at both small and large scales. The creation of a turbulent channel involves the mathematical modelling of large and small-scale eddies, as elucidated in a referenced paper [15]. This paper introduces a new model within the Gamma distribution models small-scale fluctuations, and the inverse Gamma distribution models large-scale eddies. Comparative analysis demonstrates that this new model yields results of comparable quality to the aforementioned Gamma-Gamma distribution, both in experimental and computer simulation contexts. In a related model presented in another paper [16], the Lognormal-Rician distribution was devised. Here, the Lognormal distribution was employed for modelling small-scale eddies, while the Rice distribution was utilized for modelling large-scale fluctuations. The new model demonstrated strong alignment between experimental results and outcomes obtained through software simulation.

To model and forecast the performance of free space optics (FSO) links, this paper introduces a unique model based on two statistical models. The Rician (Chi-square) distribution is employed for modelling small-scale fluctuations, while the inverse Gamma distribution is utilized for modelling large-scale eddy fluctuations [15]. The combination of these independent statistical processes results in a novel Chi-square/inverse Gamma probability density function (PDF), concurrently constituting an innovative turbulence channel [6]. Capitalizing on this, we have determined another important characterization of newly introduced turbulence model, such are cumulative distribution function (CDF) and PDF of channel signal-to-noise ratio (SNR). Further, PDF and CDF of the irradiance at the receiver under the newly introduced Chi-square/inverse

Gamma model in the presence of atmospheric turbulence and zero boresight pointing errors have been delivered. In order to conduct a full analysis of the system, the proposed model in combination with IM/DD (intensity modulation and direct detection) and OOK (on-off keying) modulation is used in this paper to determine the ABER. In such conditions, ABER has been also analysed when employing subcarrier intensity modulation (SIM) with differential phase-shift keying (DPSK). The results of the new Chi-square/inverse Gamma model are presented on tables and graphs.

The structure of the paper is as follows: Section 2 outlines the procedure for deriving the new Chi-square/inverse Gamma PDF and CDF and scrutinizes the proposed model for FSO transmission both in presence and absence of pointing errors. Section 3 delves into the presentation and analysis of performances capitalizing on delivered closed-form expressions for ABER over OOK and SIM modulation formats. Section 4 provides and discusses the results of the newly obtained model under different atmospheric turbulence conditions.

2. New turbulence model

The probability density function (PDF) of FSO fluctuations for small scale eddies is modelled using the Chi-square distribution, which is represented by the expression:

$$f_{I_x}(I_x) = \frac{1+K}{\Omega} \exp\left(-K - \frac{1+K}{\Omega} I_x\right) I_0\left(2\sqrt{\frac{K(1+K)}{\Omega} I_x}\right) \tag{1}$$

where $I_0(\cdot)$ represents the modified Bessel function of the zero order and first kind [17, Eq. 8.431], the parameter Ω represents the total received signal power, K is the Rice factor that indicates the ratio of the dominant component and the scattering component, and I_x represents irradiance at the receiver [5, 10, 11].

The PDF of FSO fluctuations of large scale eddies is modelled using the inverse Gamma distribution, represented by the expression [15]:

$$f_{I_y}(I_y) = \frac{(b-1)^b}{I_y^{b+1}\Gamma(b)} \exp\left(-\frac{b-1}{I_y}\right) \tag{2}$$

where b represents the distribution parameter, and it can be determined from the expression:

$$b = \frac{1}{\exp(\sigma_{ls}^2) - 1} + 2 \tag{3}$$

and σ_{ls}^2 can be obtained from the expression:

$$\sigma_{ls}^2 = \sigma_{ls}^2(l_0) - \sigma_{ls}^2(L_0) \tag{4}$$

and represents the log-variance of the irradiation, where $\sigma_{ls}^2(l_0)$ and $\sigma_{ls}^2(L_0)$ are the effects of fluctuations of large and small scales eddies, respectively.

$$\sigma_{ls}^2(l_0) = 0.04\,\sigma_1^2\left(\frac{\eta_{Xa}\,Q_{ls}}{\eta_{Xa}+Q_{ls}}\right)^{\frac{7}{6}}\left[1+1.75\left(\frac{\eta_{Xa}}{\eta_{Xa}+Q_{ls}}\right)^{\frac{1}{2}}-0.25\left(\frac{\eta_{Xa}}{\eta_{Xa}+Q_{ls}}\right)^{\frac{7}{12}}\right] \tag{5}$$

where:

$$\eta_{Xa} = \frac{8.56}{1+0.18a^2+0.20\,\sigma_R^2\,Q_{ls}^{1/6}} \tag{6}$$

$$Q_{ls} = \frac{10.89\,L}{k\,l_0^2} \tag{7}$$

and $k = 2\pi/\lambda$ represents the wave number, where λ is the wavelength, l_0 represents small-scale eddies (expressed in mm), while $\sigma_R^2 = 1.23\,C_n^2\,k^{7/6}\,L^{11/6}$ is Rytov variance, C_n^2 is the refractive index commonly used to define turbulence strength, and L is the distance between the transmitter and receiver.

$$\sigma_{ls}^2(L_0) = 0.04\,\sigma_1^2\left(\frac{\eta_{Xa_0}\,Q_{ls}}{\eta_{Xa_0}+Q_{ls}}\right)^{\frac{7}{6}}\left[1+1.75\left(\frac{\eta_{Xa_0}}{\eta_{Xa_0}+Q_{ls}}\right)^{\frac{1}{2}}-0.25\left(\frac{\eta_{Xa_0}}{\eta_{Xa_0}+Q_{ls}}\right)^{\frac{7}{12}}\right] \tag{8}$$

where:

$$\eta_{Xa_0} = \frac{\eta_{Xa}\,Q}{\eta_{Xa}+Q} \tag{9}$$

$$Q = \frac{64\,\pi^2 L}{k L_0^2} \tag{10}$$

and $d = \sqrt{k(2a)^2/4\,L}$ is aperture diameter, where a represents the radius of the receiver aperture, L_0 are large scale eddies and $\Gamma(\cdot)$ represents the Gamma function [17].

According to the scintillation theory [6], the received optical signal beam can be modelled as the product of two types of fluctuations $I_z = I_x I_y$, while PDF can be modelled by the expression:

$$p_{I_z}(I_z) = \int_0^\infty f_{I_x}(I_z \,|\, I_y)\, f_{I_y}(I_y)\,\mathrm{d}I_y \tag{11}$$

By substituting equations (1) and (2) into equation (11) and by representing the modified Bessel function $I_0(\cdot)$ of the zero order and first kind [17, Eq. 8.432], as the result of solved integral from [17, Eq. 3.478.4] the following equation is obtained:

$$p_{I_z}(I_z) = \sum_{p=0}^{+\infty} \frac{\Gamma(p+b+1)(b-1)^b(1+K)^{p+1}K^p\Omega^b I_z^p}{\Gamma(p+1)p!\Gamma(b)\left[(1+K)I_z+(b-1)\Omega\right]^{b+p+1}} \exp(-K) \tag{12}$$

The obtained expression represents the PDF of the Chi-square/inverse Gamma distribution.

Figure 1 shows the new distribution under weak turbulence condition, for different values of K parameter.

In order to establish the relevance of the PDF, it is necessary to determine the cumulative distribution function (CDF). The expression for calculating the CDF is given as

$$F_{I_z}(I_z) = \int_0^{\infty} p_{I_z}(I_z)\,\mathrm{d}I_z \tag{13}$$

By solving this integral, a final expression for the CDF is obtained:

$$F_z(z) = \sum_{p=0}^{+\infty} \frac{K^p \exp(-K)\Gamma(p+b+1)}{\Gamma(p+1)p!\Gamma(b)} B\left(p+1, b, \frac{(1+K)I_z}{(1+K)I_z+(b-1)\gamma}\right) \tag{14}$$

where $B(\cdot)$ denotes incomplete Beta function [17].

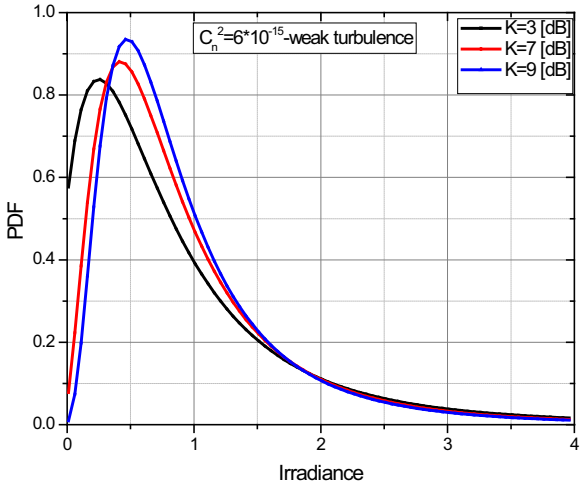

Fig. 1. PDF for the Chi-square/inverse Gamma distribution for different values of the K parameter under weak turbulence conditions.

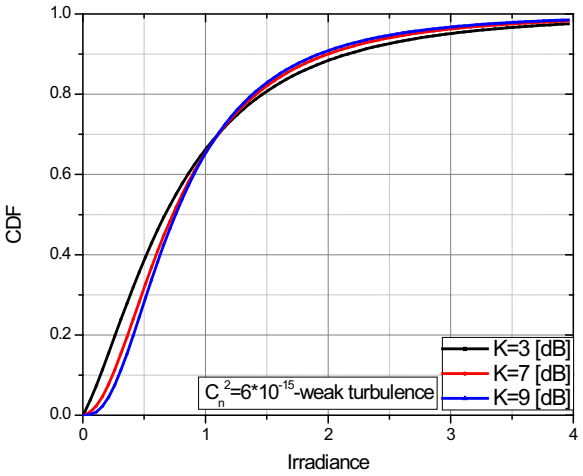

Fig. 2. CDF for the Chi-square/inverse Gamma distribution for different values of the K parameter under weak turbulence conditions.

2.1. Pointing error model

Apart from atmospheric turbulence, pointing errors exert a notable influence on the integrity of the transmitted signal. These errors result from misalignments between the transmitter and receiver. The factors contributing to pointing errors are frequently associated with thermal expansion, minor seismic activity, and the swaying of buildings caused by strong winds. In order to describe the pointing errors effect, a model presented in the literature [2] was introduced. The statement of this model is a Gaussian spatial intensity profile of optical signal attenuation w_z at the receiver surface and a circular aperture with a radius of a. Both horizontal and vertical displacements are modelled using independent Gaussian distributions, hence the radial displacement r at the receiver detector is determined by the Rayleigh distribution with jitter variance σ_s^2. The PDF of I_p is represented as:

$$f_{I_p}(I_p) = \frac{\xi^2}{A_0^{\xi^2}} I_p^{\xi^2}, \qquad 0 \le I_p \le A_0 \tag{15}$$

where $\xi = w_{L_{\text{eq}}}/2\sigma_{\text{s}}$, $w_{L_{\text{eq}}}$ is the equivalent radius of the beam at the receiver, and σ_{s} denotes the standard deviation values of the displacement error (jitter) at the receiver.

$$w_{L_{\text{eq}}}^2 = w_L^2 \frac{\text{erf}(v)\sqrt{\pi}}{2v} \exp(v^2) \tag{16}$$

where $v = \dfrac{a\sqrt{\pi}}{\sqrt{2}\, w_L}$, $A_0 = \left[\text{erf}(v)\right]^2$ and $\text{erf}(\cdot)$ denotes an error function.

Using the previous expressions, a model for stochastic FSO channels was derived, taking into account both scintillation induced by turbulence and fading caused by the misalignment between the transmitter and receiver. The PDF, $f_I(I)$ of the channel state is obtained by calculating the integral:

$$f_I(I) = \int f_I(I|I_z)\, f_{I_z}(I_z)\, \mathrm{d}I_z \tag{17}$$

where:

$$f_I(I|I_z) = \frac{1}{I_p} f_{I_p}\left(\frac{I}{I_p}\right), \qquad 0 < I \le A_0 I_z \tag{18}$$

By substituting Eqs. (12) and (15) into Eq. (17) and by solving the given integral and by applying the rules from [18, Eq. 07.23.26.0004.01] and [18, Eq. 07.34.16.0001.01], the PDF expression is obtained in the following form:

$$f_I(I) = \sum_{p=0}^{\infty} \frac{\xi^2 K^p \Gamma(b+\xi^2+1)\exp(-K)}{I(b+\xi^2)\Gamma(p+1)p!\,\Gamma(b)\Gamma(b+\xi^2)} \times G_{2.2}^{1.2}\left(\begin{matrix}1-\xi^2, -p \\ b, -\xi^2\end{matrix}\middle|\, \frac{(b-1)\Omega A_0}{(K+1)I}\right) \tag{19}$$

where $G_{p,q}^{m,n}\left(\begin{matrix}a_p \\ b_q\end{matrix}\middle| x\right)$ denotes Meijer G function.

2.2. Channel signal-to-noise ratio (SNR)

In FSO systems with IM/DD (intensity modulation and direct detection) and OOK (on-off keying) modulation schemes, the transmitted information is firstly intensity-modulated and then transmitted through the atmospheric channel. Photodetector receives optical signal whose optical power density is converted into the current and further detected. That current can be represented by the expression:

$$y_{\mathrm{T}}(t) = x(t)RI + n \tag{20}$$

where $x(t)$ denotes the signal envelope at the transmitter, the sensitivity of the photodiode is denoted by R, I denotes the intensity fluctuation of the signal, and n denotes additive white Gaussian noise (AWGN) with a zero mean and variance σ_n^2. Different noises have a significant impact on the detection of optical signals, where thermal noise, photodetector noise and background noise play particular roles. The term "white noise" originates from the uniform distribution of noise power across the frequency spectrum, analogous to the white colour, which is characterized by an even distribution of all colours in the visible spectrum. It is particularly important to note that in direct detection, the receiver responds only to the instantaneous power of the optical signal reaching the detector, without mixing with locally generated optical waves, which is

characteristic of coherent detection. The noise arising as the sum of independent and identically distributed random variables approximates a normal (Gaussian) distribution as the sample size tends to infinity. The expression for SNR can be represented as

$$\gamma = \frac{(2PRI)^2}{2\sigma_n^2} \tag{21}$$

as well as for the mean value of SNR [19]:

$$\bar{\gamma} = E[\gamma] = E\left[\frac{(2P_{\mathrm{T}}RI)^2}{2\sigma_n^2}\right] = \frac{(2P_{\mathrm{T}}R)^2}{2\sigma_n^2}E\left[I^2\right] \tag{22}$$

where $E[\cdot]$ denotes the mathematical expectation, and P_{T} is average transmitted power.

The electrical SNR is often used in the literature and can be expressed as

$$\mu = \frac{(2P_{\mathrm{T}}R)^2}{2\sigma_n^2}E^2[I] \tag{23}$$

where:

$$\gamma = \frac{\mu}{E^2[I]}I^2 \tag{24}$$

The PDF, depending on the SNR, can be obtained from the following expression:

$$f_\gamma(\gamma) = \frac{f_I(I)}{\partial\gamma/\partial I} \tag{25}$$

by substituting Eqs. (19) and (24) into Eq. (25) and applying the rules from [18, Eq. 07.34.16.0002.01], the PDF expression depending on the SNR for IM/DD with OKK modulation scheme is obtained in the following form:

$$f_\gamma(\gamma) = \sum_{p=0}^{\infty} \frac{\xi^2 K^p \Gamma(b+\xi^2+1)\exp(-K)}{2\gamma(b+\xi^2)\Gamma(p+1)p!\,\Gamma(b)\Gamma(b+\xi^2)} \times G_{2.2}^{2.1}\left(\begin{matrix}1-b,\,1+\xi^2\\ \xi^2,\,p+1\end{matrix}\middle|\,\frac{(K+1)\xi^2}{(b-1)(\xi^2+1)}\sqrt{\frac{\gamma}{\mu}}\right) \tag{26}$$

3. Performance analysis

3.1. ABER over IM/DD with OOK modulation scheme

The ABER for IM/DD with OOK modulation scheme is represented by the following expression:

$$P_{\mathrm{e}} = \frac{1}{2}\int_0^{\infty} \mathrm{erfc}\left(\frac{\sqrt{\gamma}}{2}\right) f_{\gamma}(\gamma)\mathrm{d}\gamma \tag{27}$$

where, according to [18, Eq. 06.27.26.0006.01]:

$$\mathrm{erfc}\left(\frac{\sqrt{\gamma}}{2}\right) = \frac{1}{\sqrt{\pi}} G_{1,2}^{2,0}\left(\begin{matrix}1\\ 0,\ \frac{1}{2}\end{matrix}\middle|\frac{\gamma}{4}\right) \tag{28}$$

By substituting Eqs. (26) and (28) into Eq. (27) and applying the rules from [18, Eq. 07.34.21.0013.01], the solution of the given integral is obtained, which is also the expression for ABER in SNR function for the new turbulence channel model:

$$P_{\mathrm{e}}(\mu) = \sum_{p=0}^{\infty} \frac{2^{b+p-3}\xi^2 K^p \Gamma(b+\xi^2+1)\exp(-K)}{\pi^{3/2}(b+\xi^2)\Gamma(p+1)p!\,\Gamma(b)\Gamma(b+\xi^2)} \times G_{5.4}^{3.4}\left(\begin{matrix}\frac{1-b}{2}, \frac{2-b}{2}, 1, \frac{1}{2}, \frac{2+\xi^2}{2}\\ \frac{\xi^2}{2}, \frac{p+1}{2}, \frac{p+2}{2}, 0\end{matrix}\middle|\frac{4(K+1)^2\xi^4}{(\xi^2+1)^2(b-1)^2\mu}\right) \tag{29}$$

By applying Eq. (23) in Eq. (29), the expression for ABER is obtained in the function of the transmitted average power P_{T}:

$$P_{\mathrm{e}}(P_{\mathrm{T}}) = \sum_{p=0}^{\infty} \frac{2^{b+p-3}\xi^2 K^p \Gamma(b+\xi^2+1)\exp(-K)}{\pi^{3/2}(b+\xi^2)\Gamma(p+1)p!\,\Gamma(b)\Gamma(b+\xi^2)} \times G_{5.4}^{3.4}\left(\begin{matrix}\frac{1-b}{2}, \frac{2-b}{2}, 1, \frac{1}{2}, \frac{2+\xi^2}{2}\\ \frac{\xi^2}{2}, \frac{p+1}{2}, \frac{p+2}{2}, 0\end{matrix}\middle|\frac{2(K+1)^2\sigma_{\mathrm{N}}^2}{(b-1)^2 P_{\mathrm{T}}^2 R\, A_0^2 \Omega^2}\right) \tag{30}$$

3.2. ABER expression for SIM modulation

The intensity of the optical signal when using SIM modulation can be represented by the following expression:

$$I_{\mathrm{S}} = P(1 + m\,s(t)) \tag{31}$$

where P is the average optical power, m is the modulation index, and $s(t)$ is the signal from the electrical modulator. After the transmission of the signal through the channel and by applying direct detection at the receiver, the electrical signal can be represented by the following expression:

$$y_{\mathrm{T}}(t) = x(t)RPmI + n \tag{32}$$

where n denotes AWGN with a zero mean and a variance σ_n^2. The expression for SNR can be represented as:

$$\gamma = \frac{(RPmI)^2}{2\sigma_n^2} \tag{33}$$

as well as for the mean value of SNR [19]:

$$\bar{\gamma} = E[\gamma] = E\left[\frac{(RPmI)^2}{\sigma_n^2}\right] = \frac{(RPm)^2}{2\sigma_n^2} E\left[I^2\right] \tag{34}$$

the expression for electrical SNR can be represented as:

$$\mu = \frac{(RPm)^2}{2\sigma_n^2} E^2[I] \tag{35}$$

where:

$$\gamma = \frac{\mu}{E^2[I]} I^2 \tag{36}$$

The expression for ABER when using SIM modulation with direct detection with respect to the current electrical SNR can be represented as [20]:

$$P_{\mathrm{e}} = \frac{1}{2}\int_0^{\infty} Q(\sqrt{2\gamma}\,) f_{\gamma}(\gamma)\,\mathrm{d}\gamma \tag{37}$$

where $Q(\cdot)$ denotes the Gaussian Q-function:

$$Q(x) = \frac{1}{2}\operatorname{erfc}(x) \tag{38}$$

By solving the integral from Eq. (37) using Eq. (19), which is adjusted by the rule [18, Eq. 07.34.16.0002.01], and Eq. (38), which can be represented through the Mayer function using [18, Eq. 06.27.26.0006.01], as well as by applying Eqs. (25) and (34), the expression that represents ABER for SIM modulation is obtained:

$$P_{\text{e sim}}(\mu) = \sum_{p=0}^{\infty} \frac{2^{b+p-3}\xi^2 K^p \Gamma(b+\xi^2+1)\exp(-K)}{\pi^{3/2}(b+\xi^2)\Gamma(p+1)p!\,\Gamma(b)\Gamma(b+\xi^2)}$$

$$\times G_{5.4}^{3.4}\left(\left.\begin{matrix}\frac{1-b}{2}, \frac{2-b}{2}, 1, \frac{1}{2}, \frac{2+\xi^2}{2} \\ \frac{\xi^2}{2}, \frac{p+1}{2}, \frac{p+2}{2}, 0\end{matrix}\right| \frac{(K+1)^2\xi^4}{(\xi^2+1)^2(b-1)^2\mu}\right) \tag{39}$$

4. Numerical results

For the implementation of experimental results, the parameters from the Table 1 are used. The remaining values of the parameters are presented in the paper.

T a b l e 1. Values of the parameters used for numerical calculations.

Parameters description	Value
Refractive index - turbulence strength C_n^2	6×10^{-15} m$^{-2/3}$ (weak), 2×10^{-14} m$^{-2/3}$ (moderate), 1.2×10^{-13} m$^{-2/3}$ (strong)
Wavelength λ	1000 nm
Distance between transmitter and receiver L	950 m
Total received signal power Ω	1 W
Detector responsivity R	1 A/W
Noise standard deviation σ_n	10^{-7} A/Hz
Radius of a circular detector aperture a	0.05 m
Radius at the distance L from transmitter w_L	0.6 m
Outer scale effects L_0	0.8 m
Inner scale effects l_0	6 mm

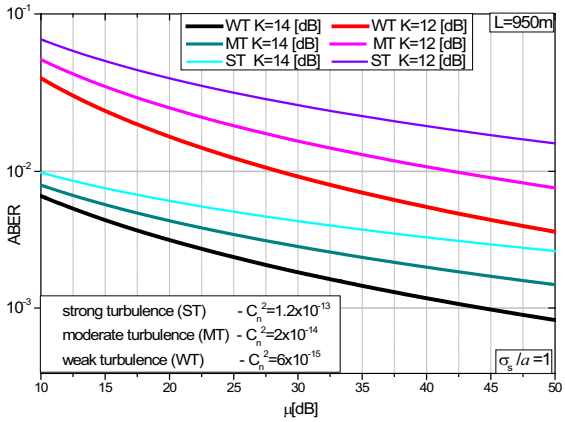

Fig. 3. ABER for the Chi-square/inverse Gamma model as a function of the average electrical SNR.

Utilizing the formula (29) for the recently formulated turbulence channel Chi-square/inverse Gamma at Fig. 3, ABER versus channel SNR (μ) was depicted for the IM/DD with OOK scheme. Different levels of atmospheric turbulence strengths and K factors were taken into account in the determination of ABER.

As expected, under conditions of strong turbulence and for smaller values of the K parameter, the ABER value is higher. As the turbulences strength decreases so does the value of ABER. For values of weak turbulence and higher values of K parameter, the ABER value reaches its lowest levels. It can be observed, that the increase of the electrical SNR leads to a linear decrease in ABER. The FSO system has the best performances (lowest ABER) under conditions of weak turbulence and for the highest values of the K parameter, while the performances are the poorest when strong turbulence is present and the value of K parameter is lowest.

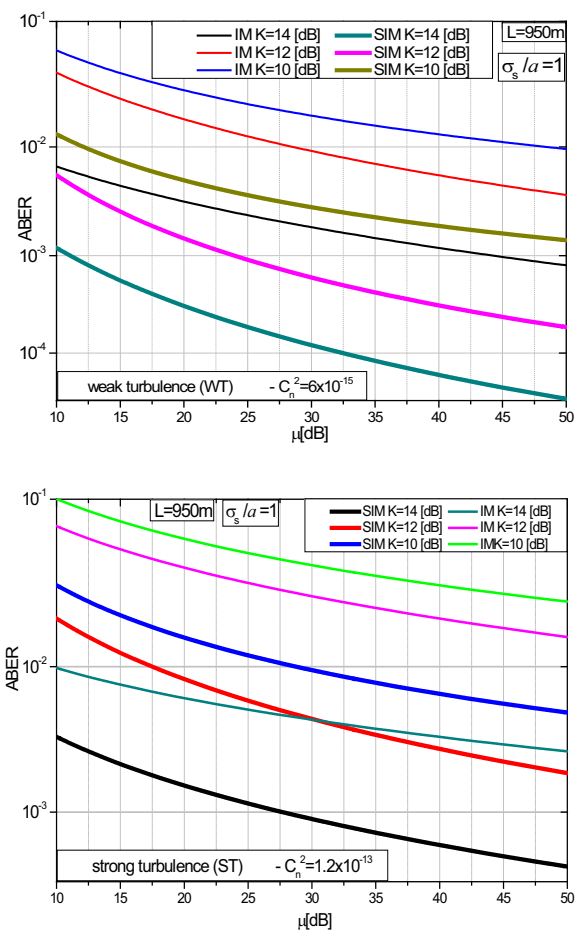

Fig. 4. ABER for the Chi-square/inverse Gamma model in conditions of weak turbulence when using SIM and IM/DD with OOK modulation as a function of electrical SNR (a), and strong turbulence when using SIM and IM/DD with OOK modulation as a function of electrical SNR (b).

Figures 4(a) and (b) compare the dependence of ABER on electrical SNR when using IM/DD with OOK modulation and SIM modulation.

The existing findings for IM/DD with OOK modulation, indicating enhanced system performance with reduced turbulence and increased K factor, are equally applicable to SIM modulation. The graphical representations manifest superior characteristics of SIM modulation across diverse atmospheric turbulence conditions and K factor values. Furthermore, a discernible trend reveals that as the electrical SNR intensity rises, the performance distinction diminishes.

Zero boresight pointing error influence over newly derived turbulence channel Chi-square-inverse Gamma was observed through ABER and the average transmitted optical power P_T for different values of jitter deviation at Fig. 5(a).

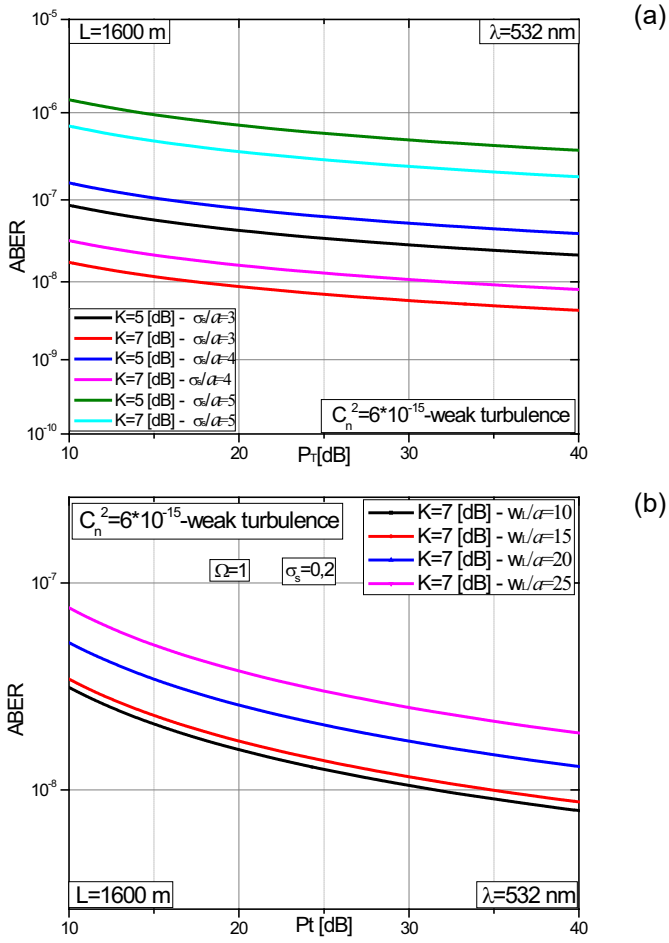

Fig. 5. ABER for the Chi-square/inverse Gamma zero boresight pointing error channel model for different values of the normalized standard jitter deviation (a), and different values of the normalized optical beam radius (b).

Figure 5(a) shows that with an increase in the transmitted power ABER decreases linearly. It can be concluded that for smaller values of jitter deviation, ABER is lower, and as the jitter deviation increases, ABER also increases. However, increasing in the K factor can mitigate the increase in ABER caused by higher jitter deviation. Incorrect transmitter-receiver alignment results in an increase in the jitter deviation, which leads to system performance degradation.

Figure 5(b) shows ABER as a function of transmitted power for different values of the optical beam radius under conditions of weak turbulence. Given that a larger value of the optical beam radius w_L is conditioned by the increase in the distance of the transmitter depending on the radius of the detector a, it leads to the fact that an increase in w_L also increases ABER. A smaller ratio between the optical beam width and the radius of the detector results in a decrease of ABER.

5. Conclusion

This manuscript introduces a novel turbulence model for FSO communication, crafted through the integration of two distinct statistical models rooted in the scintillation theory. The derived closed-form expression for PDF and CDF of the turbulence channel, specifically the Chi-square/inverse Gamma distribution, contributes to the understanding of FSO signal characteristics. The study expands its scope to investigate the impact of zero boresight pointing errors on FSO transmission performance over the obtained atmospheric turbulence channel. ABER evaluations are conducted within the framework of IM/DD with OOK and SIM with DPSK, considering diverse system parameters and turbulence scenarios. The paper extends the discourse on turbulence modelling, introducing a comprehensive perspective on the Chi-square/inverse Gamma distribution, scintillation theory, zero boresight pointing errors, and ABER. The utilization of mathematical models for signal intensity in turbulent channels is critical, and the presented research acknowledges the diversity of atmospheric conditions, requiring specific models and approaches for accurate representation. The obtained results, presented through graphs, provide insights into the performance of the proposed model under various atmospheric turbulence conditions.

References

[1] FARID A.A., HRANILOVIC S., *Outage capacity optimization for free-space optical links with pointing errors*, Journal of Lightwave Technology **25**, 2007: 1702-1710. https://doi.org/10.1109/JLT.2007.899174

[2] LI J., UYSAL M., *Achievable information rate for outdoor free space optical communication with intensity modulation and direct detection*, Global Telecommunications Conference, 2003: 2654-2658. https://doi.org/10.1109/GLOCOM.2003.1258717

[3] GARRETT I., *Pulse-position modulation for transmission over optical fibers with direct or heterodyne detection*, IEEE Transactions on Communications **31**(4), 1983: 518-527. https://doi.org/10.1109/TCOM.1983.1095842

[4] POPOOLA W.O., *Subcarrier Intensity Modulated Free-space Optical Communication Systems*, Doctoral Thesis, Northumbria University, 2009.

[5] Belmonte A., Kahn J.M., *Performance of synchronous optical receivers using atmospheric compensation techniques*, Optics Express **16**(18), 2008: 14151-14162. https://doi.org/10.1364/OE.16.014151

[6] Wang N., Cheng J., *Moment-based estimation for the shape parameters of the Gamma-Gamma atmospheric turbulence model*, Optics Express **18**(12), 2010: 12824-12831. https://doi.org/10.1364/OE.18.012824

[7] Nistazakis H.E., Assimakopoulos V.D., Tombras G.S., *Performance estimation of free space optical links over negative exponential atmospheric turbulence channels*, Optik **122** (24), 2011: 2191-2194. https://doi.org/10.1016/j.ijleo.2011.01.013

[8] Popoola W.O., Ghassemlooy Z., Ahmadi V., *Performance of sub-carrier modulated free-space optical communication link in negative exponential atmospheric turbulence environment*, International Journal of Autonomous and Adaptive Communications Systems **1**(3), 2008: 342-355. https://doi.org/10.1504/IJAACS.2008.019809

[9] Youssef N., Munakata T., Takeda M., *Fade statistics in Nakagami fading environments*, Proceedings of ISSSTA'5 International Symposium on Spread Spectrum Techniques and Applications, Mainz, Germany, Vol. 3, 1996: 1244-1247. https://doi.org/10.1109/ISSSTA.1996.563504

[10] Sandalidis H.G., Tsftsis T.A., Karagiannidis G.K., Uysal M., *BER performance of FSO links over strong atmospheric turbulence channels with pointing errors*, IEEE Communications Letters **12**(1), 2008: 44-46. https://doi.org/10.1109/LCOMM.2008.071408

[11] Prlincevic B.P., Milovanovic B.D., Spalevic P.C., Panic S.R., Milivojevic Z.N., *Perfomance analysis of FSO transmission of watermarked image over Rician fading channels*, 2015 12th International Conference on Telecommunication in Modern Satellite, Cable and Broadcasting Services (TELSIKS), Nis, Serbia, 2015: 72-75. https://doi.org/10.1109/TELSKS.2015.7357740

[12] Hodara H., *Laser wave propagation through the atmosphere*, Proceedings of the IEEE **54**(3), 1966: 368-375. https://doi.org/10.1109/PROC.1966.4698

[13] Hassan M., *On the Performance of Non-Adaptive and Adaptive Optical Wireless Communications in Atmospheric Turbulence*, PhD Dissertation, The University of British Columbia, Okanagan, 2013.

[14] Arnon S., Barry J., Karagiannidis G., *Advanced Optical Wireless Communication Systems*, Cambridge University Press, 2012.

[15] Peppas K.P., Alexandropoulos G.C., Xenos E.D., Maras A., *The Fischer–Snedecor F-distribution model for turbulence-induced fading in free-space optical systems*, Journal of Lightwave Technology **38**(6), 2019: 1286-1295. https://doi.org/10.1109/JLT.2019.2957327

[16] Yang F., Cheng J., *Coherent free-space optical communications in lognormal–Rician turbulence*, IEEE Communications Letters **16**(11), 2012: 1872-1875. https://doi.org/10.1109/LCOMM.2012.100812.121341

[17] Gradshteyn I.S., Ryzhik I.M., *Table of Integrals, Series, and Products*, 7th Ed., Elsevier Academic Press, 2007.

[18] https://mathworld.wolfram.com

[19] Niu M., Cheng J., Holzman J.F., *Error rate performance comparison of coherent and subcarrier intensity modulated optical wireless communications*, Journal of Optical Communications and Networking **5**(6), 2013: 554-564. https://doi.org/10.1364/JOCN.5.000554

[20] Ghassemlooy Z.F., Popoola W.O., Leitgeb E., *Free-space optical communication using subcarrier modulation in gamma-gamma atmospheric turbulence*, 9th International Conference on Transparent Optical Networks (ICTON), Vol. 3, 2007: 156-160.

Received February 3, 2024
in revised form April 7, 2024